Published in final edited form as:

Nature. 2018 March 15; 555(7696): 377–381. doi:10.1038/nature25975.

Human hippocampal neurogenesis drops sharply in children to undetectable levels in adults

Shawn F. Sorrells[1,2,*], **Mercedes F. Paredes**[1,3,*], **Arantxa Cebrian-Silla**[4], **Kadellyn Sandoval**[1,3], **Dashi Qi**[5], **Kevin W. Kelley**[1], **David James**[1], **Simone Mayer**[1,3], **Julia Chang**[6], **Kurtis I. Auguste**[2], **Edward Chang**[2], **Antonio J. Gutierrez Martin**[7], **Arnold R. Kriegstein**[1,3], **Gary W. Mathern**[8], **Michael C. Oldham**[1,2], **Eric J. Huang**[9], **Jose Manuel Garcia-Verdugo**[4], **Zhengang Yang**[5], and **Arturo Alvarez-Buylla**[1,2]

[1]Eli and Edythe Broad Center of Regeneration Medicine and Stem Cell Research, University of California San Francisco, California 94143, USA

[2]Department of Neurological Surgery, University of California San Francisco, California 94143, USA

[3]Department of Neurology, University of California San Francisco, California 94143, USA

[4]Laboratorio de Neurobiología Comparada. Instituto Cavanilles. Universidad de Valencia, CIBERNED, Valencia, 46980, Spain

[5]State Key Laboratory of Medical Neurobiology and Institutes of Brain Science, Department of Neurology, Zhongshan Hospital, Fudan University, Shanghai, P.R. 200032 China

[6]David Geffen School of Medicine, Department of Neurosurgery, Intellectual Development and Disabilities Research Center, University of California Los Angeles, California USA

[7]Unidad de Cirugía de la Epilepsia, Hospital Universitario La Fe, Valencia 46026, Spain

[8]Departments of Neurosurgery and Psychiatry & BioBehavioral Medicine, David Geffen School of Medicine, University of California Los Angeles, California USA

[9]Department of Pathology, University of California San Francisco, California 94143, USA

Abstract

Materials & Correspondence. Correspondence and requests for materials should be addressed to A.A.-B. at AlvarezBuyllaA@ucsf.edu, Z.Y. at yangz@fudan.edu.cn, or J.G.-V. at j.manuel.garcia@uv.es.

Supplementary Information is linked to the online version of the paper at www.nature.com/nature

Author contributions. M.F.P. and S.F.S. contributed equally as co-first authors and A.C.-S., K.S., and D.Q. contributed equally as second authors. Z.Y., A.A.-B., M.F.P. and S.F.S. conceived the study and A.A.-B., S.F.S., and M.F.P. designed and interpreted the experiments and with A.C.-S., K.S., D.Q., S.M. and D.J. conducted the experiments. K.I.A., E.C., J.C., E.J.H., A.J.G.-M., A.R.K. and G.W.M. assisted with specimen collection and conducted clinical and neuropathological review. K.K. and M.C.O. designed and performed the bioinformatic analyses. A.C.-S. and J.M.G.-V. conducted and interpreted the ultrastructural studies. S.F.S., M.F.P., A.C.-S. and K.S. prepared the figures. A.A.-B., S.F.S. and M.F.P. wrote the manuscript with input from all authors.

Data Availability. All data generated during and/or analyses during the current study are available from the corresponding author.

Competing financial interests. The authors declare no competing financial interests.

New neurons continue to be born in the subgranular zone (SGZ) in the dentate gyrus (DG) of the adult mammalian hippocampus[1–5]. This process has been linked to learning and memory, stress and exercise, and is thought to be altered in neurological disease[6–10]. In humans, some studies suggest that hundreds of new neurons are added to the adult DG every day[11], while other studies find many fewer putative new neurons[12–14]. Despite these discrepancies, it is generally believed that the adult human hippocampus continues to generate new neurons. Here we show that a defined population of progenitor cells does not coalesce in the SGZ during human fetal or postnatal development. We also find that proliferating progenitors and young neurons in the DG sharply decline in the first year of life and only a few isolated young neurons are observed by 7 and 13 years of age. In adult normal and epileptic patients(18–77 years; n=17 postmortem; n=12 epilepsy), young neurons were not detected in the DG. In the monkey (*M. mulatta*) hippocampus, a proliferative SGZ was present in early postnatal life, but diminished during juvenile development as neurogenesis declined. We conclude that recruitment of young neurons to the primate hippocampus declines rapidly during the first years of life, and that DG neurogenesis does not continue, or is extremely rare, in the adult human. The early decline in hippocampal neurogenesis raises questions about how the function of the dentate gyrus differs between humans and other species in which adult hippocampal neurogenesis is preserved.

We used 59 postmortem and intraoperative samples of the human hippocampus (Supplementary Table 1) to investigate the presence of progenitor cells and young neurons from fetal to adulthood stages. At 14 gestational weeks, at the peak of proliferation in the fetal dentate gyrus (DG)[15], many dividing (Ki-67+) neural progenitors (SOX1+ (ref. 16) and SOX2+ (ref. 17)) were observed in the dentate neuroepithelium (dNE; Fig. 1a, Extended Data Fig. 1a–c and Supplementary Video 1). A continuous field of Ki67+SOX1+ and Ki67+SOX2+ cells, associated with ribbons of Nestin+Vimentin+ fibers and cells, was observed between the dNE and the proximal blade of the DG. At 22 GW, the proliferating cells between the dNE and the DG greatly diminished, and most Ki67+SOX1+ or Ki67+SOX2+ cells in the hippocampus were found in the hilus (Fig. 1b, Extended Data Fig. 1d–f). By this age, most young neurons (DCX+PSA-NCAM+ cells), were concentrated in the granule cell layer (GCL) proximal to the dNE (Fig. 1c). The distal GCL, in contrast, contained higher numbers of mature NeuN+ neurons (Extended Data Fig. 1g,h), suggesting a gradient of maturation.

To look for the formation of a proliferative SGZ, we characterized dividing and progenitor cells in the human DG from fetal development to adulthood. At 22 GW, Ki67+ cells were predominantly observed in the hilus and next to the distal GCL (Fig. 1b, 2a). By early postnatal life Ki67+ cells remained distributed throughout the hilus and GCL (Fig. 2a). The number of Ki-67+Sox1+ or Ki-67+Sox2+ cells decreased in the hilus during the first year of life (Fig. 2b–d), but these cells did not form a discrete layer beneath the GCL at any of the ages studied (Fig. 2a–d). There were rare instances of SOX2+ Ki67+ cells in the 35 year old DG, but these cells were BLBP- and were dispersed throughout the hippocampus. Light and electron microscopy at 22 GW, birth, 7, 18 and 48 years did not reveal a layer of cells with progenitor characteristics adjacent to the GCL (Extended Data Figs. 2a–c, 3). Ki67+BLBP+ cells were found in the developing DG during fetal and early postnatal stages, but BLBP+ cells were Ki67- in juvenile and adult brains and were primarily in the molecular layer (ML)

(Extended Data Figs. 2b). Furthermore, immunostaining for nestin, vimentin or GFAP in brain sections from individuals that were 7 years of age and older did not show cells next to the DG or in the hilus that had the typical neural progenitor/stem cell morphology of radial astrocytes (also known as radial or type-I cells)[3,4,18]. BLBP and Vimentin became depleted from the hilus and were predominantly expressed in mature stellar astrocytes in the ML by 7 years and in older brains. GFAP-expressing cells that remained in the adult hilus were stellate ALDH1L1+ astrocytes with thin fibers extending through the hilus and GCL (Extended Data Figs. 3a,d, 4). These cells were not Ki67+ or found in mitosis. These results indicate that a germinal SGZ does not form next to the human DG, and proliferating cells expressing progenitor/stem cell markers become largely depleted from the hilus by 7 years of age.

We next looked for the presence of young neurons in the human DG. At birth DCX+PSA-NCAM+ cells were located across the GCL, frequently in clusters (Fig. 3a,b). The number of DCX+PSA-NCAM+ cells in the GCL declined from 1,618 (SD ±780) cells/mm^2 at birth to 292.9 (SD ±142.8) cells/mm^2 at 1 year of age. By 7 years of age, 12.4 ± 5.3 DCX+PSA-NCAM+ cells per mm^2 were found in the GCL and at 13 years of age, the GCL contained 2.4 ± 0.74 DCX+PSA-NCAM+ cells per mm^2 (that is, approximately 1–2 DCX+PSA-NCAM+ cells per section; Fig. 3c–e and Extended Data Fig. 5). DCX+ cells in the infant (≤ 1 year) DG not only expressed PSA-NCAM, but also frequently had the simple elongated morphology of young neurons (Extended Data Fig. 5b). In contrast, light and electron microscopy at 7 years showed DCX+ cells in different stages of maturation (Extended Data Fig. 6a). DCX+ cells in the hippocampus of a 13-year-old individual had a more mature morphology (Fig. 3e), expressed NeuN and had distinct axons and dendrites (Extended Data Fig. 5c). We examined 17 adult postmortem hippocampi between the ages of 18-77 years (Supplementary Table 1) to look for evidence of young neurons. In two adults (sample numbers 24 and 26), we also studied the ventricular wall and found rare DCX+ cells with a migratory morphology in the ventricular–subventricular zone [19,20], providing a positive control (Extended Data Fig. 6b). We found no evidence of DCX+PSA-NCAM+ young neurons in the hilus or GCL of the hippocampi from these cases,(Extended Data Figs. 5d, 6b). At 3 weeks of age there were many DCX+Tuj1+ labeled young neurons in the GCL, however we did not detect these cells at 19 or 36 years of age. In adults, we observed Tuj1+ fibers belonging to many mature neurons (Extended Data Fig. 6c). PSA-NCAM+ cells were present in the hilus and GCL of adult brains, but these cells had a mature neuronal morphology and were NeuN+ (Extended Data Fig. 5b, d–f). Using single-molecule in situ hybridization labelling of DCX transcripts, we detected many DCX+ cells in the GCL at 14 gestational weeks, but only weak signal in very few, widely distributed cells at 13 years (Extended Data Fig. 6d). A subpopulation of cells with round nuclei were occasionally labeled by DCX antibodies. These DCX+ cells had multiple processes, were not restricted to the hippocampus, expressed the glial markers Iba1 or Olig2, and had ultrastructural features of glia (Extended Data Fig. 7).

We also examined progenitor cell proliferation and the presence of young neurons in surgical resections containing the hippocampus from epilepsy cases (Supplementary Table 1). In these samples, Ki-67+BLBP+SOX2+ or Ki-67+SOX1+vimentin+ cells were present in the hilus and GCL of a 10-month-old individual, but were absent from the sample of an

11-year-old individual (Extended Data Fig. 8a, b). We also found many DCX+PSA-NCAM+ cells at 10 months, whereas only a few cells per section were found in samples from a 7-year-old individual and none were found in 13 surgical resections from individuals that were older than 11 years of age (Extended Data Fig. 8c–g). There was no evidence of a discrete layer of dividing cells or young neurons in any of the adult epilepsy cases studied.

We next analyzed proliferative progenitors and young neurons in the macaque monkey (*Maccaca mulatta).* Early studies using thymidine-labeling found no evidence of new-born neurons in adults (17 year old), but subsequent work using injections of BrdU (a thymidine analogue that labels newly born cells) suggested low levels of neurogenesis, even in the 23 year old monkey DG[2,21]. At embryonic day (E) 150, remnants of the migratory stream between the dNE and the proximal blade of the developing DG were observed (Extended Data Fig. 9a). Ki67+ and DCX+ cells consolidated into a layer in the SGZ between embryonic day 150 (E150) and birth (Fig. 4, Extended Data Fig 9a–c). Between birth and 1.5 years, the number of Ki67+ cells decreased 8-fold and the macaque SGZ became less defined (Fig. 4a). The average number of proliferating cells decreased 35-fold between 1.5 and 7 years of age (Fig. 4e). A continuous SGZ was not detected in macaques that were older than 7 years. Instead, isolated small dark cells and occasional Ki67+ cells were observed next to the GCL (Fig. 4a, Extended Data Fig. 9b). Similarly, the number of DCX +PSA-NCAM+ young neurons decreased during this period, becoming sparse and discontinuous by 7 years of age (Fig. 4b–d, f). Most DCX+PSA-NCAM+ cells at 5 years and older had round nuclei and extensive dendritic trees (Fig. 4c,d, Extended Data Fig. 9d), but some retained the elongated morphology and ultrastructure of young neurons (Fig. 4d,g). While DCX+ cells in the 23 year old macaque DG were rare, they were readily found in the V-SVZ and RMS[22] (Extended Data Fig. 9e). We next used BrdU to label recently dividing cells in two 1.5-year-old macaques; at this age the SGZ contained markers of progenitors and young neurons (Extended Data Fig. 9f,g). We allowed 10 and 15 week survival after 5 days of twice-daily BrdU (50mg/kg) injections. DCX+BrdU+ and a few NeuN+BrdU+ cells were observed in the SGZ and GCL (Extended Data Fig. 9h,i Supplementary Table 4). By contrast, in the brains of 7-year-old macaques that received the same BrdU treatment, we found no DCX+BrdU+ cells in the SGZ 10 weeks after BrdU treatment; 15 weeks after BrdU treatment, we found two DCX+BrdU+ cells (Extended Data Fig. 9j and Supplementary Table 4). We did not find BrdU+NeuN+ cells in the GCL of these 7 year old monkeys. Given the higher level of neurogenesis observed in the 1.5 year old macaque, we studied one monkey at this age with a 2 hour survival after a single BrdU injection. Many BrdU+ cells that expressed the proliferative markers, Ki-67 and MCM2, and the progenitor marker, SOX2, were present in the SGZ (Extended Data Fig. 9h). Finally, we compared hippocampal gene expression profiles from macaque and human (Extended Data Fig. 10). A sharp decline in DCX, TUJ1, and Ki67 expression was observed in both species. In normalized developmental time, the decline in DCX-expressing cells was accelerated in human compared to macaque (Extended Data Fig. 10). We conclude that there is a dramatic decrease in neurogenesis in the macaque DG during juvenile ages, with rare DCX+PSA-NCAM+ young neurons in adults.

In the rodent brain, a proliferative SGZ consolidates around P10[23,24], and neural stem cells within this region continue to generate new neurons into adulthood[4]. In the human brain,

however, we did not find an equivalent proliferative region at any of the ages analysed. Ki67+ cells were distributed throughout the fetal and infant hilus and GCL. The adult human SGZ was devoid of precursor cells and young neurons, and instead contained many ALDH1L1+GFAP+ cells. It is intriguing that we found rare examples of SOX2+ Ki67+ cells in the adult DG, but these cells were not confined to the hilus or GCL and were BLBP-. We cannot exclude the possibility that neural stem cells in humans are BLBP- or are highly dispersed, but we did not observe DCX+ PSA-NCAM+ cells in these same samples. The simplest explanation is that these cells are dividing local glia, many of which are known to express SOX2+[25,26] Extended Data Fig. 3c). The lack of a coalesced SGZ could explain the absence (or rarity) of DG neurogenesis in the adult human brain.

The above findings do not support the notion that robust adult neurogenesis continues in the human hippocampus (see extended discussion). ^{14}C birthdating on sorted NeuN+ nuclei[11] has suggested that many new neurons continue to be generated in the adult human hippocampus, with little decline with age, but additional evidence for high levels of progenitors or young neurons was not shown. Interestingly, considerable interindividual variation was observed in this study, and many individual samples had ^{14}C levels consistent with no, or little, postnatal neuronal addition. Labeled neuronal cells in the GCL in patients that received a low dose of BrdU[13], could possibly be explained by processes not associated with cell division[27,28] (Extended Data Fig. 7f). Other groups find a sharp decline with age in proliferation and markers of DG neurogenesis[12,14,29], consistent with the above findings. It has been suggested that a few new neurons continue to be produced in adults based on DCX expression detected by PCR or western blot[14,29,30]. However, glial cells can express DCX[26] (Extended Data Fig. 7c–e), possibly explaining some of these expression data. The lack of young neurons in our adult human DG samples could be due to processes linked to disease and/or death. Similar results were obtained in DG from intraoperative samples or from patients with diverse causes of death. In contrast, young neurons were found in epilepsy samples from children and in our control pediatric cases, despite diverse clinical histories. Unlike in humans, we observed a germinal SGZ in the young macaque. We found that neurogenesis continues postnatally in macaques, but like humans, this process declined in juveniles and adults, consistent with previous ^{3}H-thymidine- and BrdU-studies[2,21,31]. If neurogenesis continues in the adult human hippocampus, this is a rare phenomenon, raising questions of how human dentate gyrus plasticity differs from other species in which adult hippocampal neurogenesis is abundant. Interestingly, a lack of neurogenesis in the hippocampus has been suggested for aquatic mammals (dolphins, porpoises and whales)[5], species known for their large brains, longevity and complex behavior. Understanding the limitations of adult neurogenesis in the human and other species is fundamental to interpreting findings from animal models.

Methods

Human tissue collection

Thirty-seven post-mortem specimens from controls and twenty-two post-operative neurosurgical specimens from patients with epilepsy were collected for this study (Supplementary Table 1). Tissue was collected with previous patient consent in strict

observance of the legal and institutional ethical regulations in accordance with each participating institution: 1. The University of California, San Francisco (UCSF) Committee on Human Research. Protocols were approved by the Human Gamete, Embryo and Stem Cell Research Committee (Institutional Review Board) at UCSF. 2. The Ethical Committee for Biomedical Investigation, Hospital la Fe (2015/0447) and the University of Valencia Ethical Commission for Human Investigation. 3. In accordance with institutional guidelines and study design approval by the institutional review board (Ethics Committee) of Shanghai Medical College (20110307-085, 20120302-099). 4. Specimens collected at UCLA had IRB approved research informed consents along with HIPAA authorizations signed by parents or responsible guardians, as per the UCLA Human Research Protection Program. For infant cases, when the brain is at full term (37 to 40 gestational weeks) and autopsy performed within 2 days after birth, we refer to this as “birth”. We collected tissue blocks from the temporal lobe, posteriorly from the amygdaloid complex to the posterior end of the inferior horn of the lateral ventricle. Autopsy samples had a post-mortem interval of less than 48 h, and samples from patients with epilepsy had less than 1 h to fixation (in 4% paraformaldehyde (PFA) or 10% formalin). For two adult brains (35-years old and 39-years old), the individuals were perfused within 3–5 h of death with 4% PFA during autopsy via the carotid artery and placed in fixative. All brains were typically cut into ~1.5 cm blocks, fixed in 4% PFA for an additional 2 days, cryoprotected in a 30% sucrose solution, and then frozen in embedding medium, OCT. Blocks were cut into 30 micron sections on a cryostat and mounted on glass slides for immunohistochemistry. For each case, we cresyl-stained a minimum of 3 sections at different levels to confirm anatomical landmarks and orientation. Neurosurgical excisions of temporal lobe which included hippocampus were performed as part of resection treatment in patients with intractable epilepsy as previously described[32]. We recorded the anatomical origin of each intra-operative specimen with intra-operative neuronavigation. Intra-operative specimen assessments were independently confirmed by a neuropathologist. We performed immunohistochemistry staining on surgical sections to look for the expression of PROX1 to confirm the location of the GCL.

Macaque tissue preparation

All animal care and experiments were conducted in accordance with the Fudan University Shanghai Medical College and UC Davis guidelines. Embryonic, neonatal, juvenile and adult macaque monkeys, Macaca mulatta, of both sexes at various ages (Supplementary Table 2), were obtained from the Kunming Primate Research Center of Chinese Academy of Sciences at Kunming, China, Suzhou Xishan Zhongke Laboratory Animal Co., Ltd., Suzhou, China and the UC Davis Primate Research Center. For immunohistochemical staining, postnatal monkeys were deeply anesthetized and then perfused with PBS followed by 4% PFA. The brains were removed and postfixed with 4% PFA for 12–48 h. Postnatal brains were then cut coronally into approximately 1.0- to 2.0-cm slabs and cryoprotected in 30% sucrose in 0.1 M phosphate buffer at 4°C for 72 h. The brain tissue samples were frozen in embedding medium (OCT) on a dry ice and ethanol slush.

BrdU administration

We used 5 monkeys to do BrdU labeling experiments: three 1.5 year old monkeys, and two 7-7.5 year old monkeys. BrdU acute labeling: One 1.5 year old monkey was injected once

intravenously with BrdU (50 mg/kg) and sacrificed 2 hours after BrdU injection. BrdU birth dating: BrdU (50 mg/kg) was injected intravenously twice daily for 5 days, to two 1.5 year old monkeys, and two 7-7.5 year old monkeys. One 1.5 year old and one 7 year old monkey were sacrificed 10 weeks after BrdU injections; another 1.5 year old and one 7.5 year old monkey were sacrificed 15 weeks after BrdU injections. 52 sections were analyzed for the presence of BrdU-labeling in the 7.5 year macaque with 10 week delay; in the 7 year with 15 week delay, 76 sections were analyzed.

Immunohistochemistry

Frozen slides were allowed to equilibrate to room temperature for 3 hours. Some antigens required antigen retrieval (Supplementary Table 3), which was conducted at 95°C in 10 mM Na citrate buffer, pH=6.0. Following antigen retrieval, slides were washed with TNT buffer (0.05% TX100 in PBS) for 10 minutes, placed in 1% H2O2 in PBS for 45 minutes and then blocked with TNB solution (0.1 M Tris-HCl, pH 7.5, 0.15 M NaCl, 0.5% blocking reagent from PerkinElmer) for 1 hour. Slides were incubated in primary antibodies overnight at 4°C (Supplementary Table 3) and in biotinylated secondary antibodies (Jackson Immunoresearch Laboratories) for 2.5 hours at room temperature. All antibodies were diluted in TNB solution. For most antibodies, the conditions of use were validated by the manufacturer (antibody product sheets). When this information was not provided, we performed control experiments, including no primary antibody (negative) controls and comparison to mouse staining patterns.

Sections were then incubated for 30 min in streptavidin-horseradish peroxidase that was diluted (1:200) with TNB. Tyramide signal amplification (PerkinElmer) was used for some antigens. Sections were incubated in tyramide-conjugated fluorophores for 5 minutes at the following dilutions: Fluorescein: 1:50; Cy3: 1:100; Cy5: 1:100. For sections that used the 3', 3'-diaminobenzidine (DAB) chromagenic IHC method, the sections were first rinsed in PBS, incubated for 15 min in 1% H2O2, then incubated for 2 hours in 10% fetal calf serum as the blocking buffer. This was followed by overnight incubation with the primary antibody at 4°C, followed by incubation with the secondary antibody for 2 h at room temperature, and development using the VECTASTAIN ABC HRP system (Vector Laboratories). After several PBS rinses, sections were dehydrated, mounted and coverslipped. Staining was conducted in technical triplicates prior to analysis.

Fluorescent microscopy, image processing and quantifications

Images were acquired on Leica TCS SP8 or SP5 confocal microscopes using 10x (0.3 NA) or 63x (1.4 NA) objective lenses. Imaging of entire sections and for quantification of DCX +PSA-NCAM+ cells was at 20x (0.45 NA) on a Zeiss Axiovert 200M microscope or Keyence BZ-X Analyzer (BZX700) and individual files stitched automatically. Imaging files were analyzed and quantified in Neurolucida software (MBF Bioscience 2017 version). Linear adjustments to image brightness and contrast were made equivalently across all images using Adobe Photoshop (CS 6). Cells were counted in Z-stack images from sections stained with Ki-67 and SOX2 or DCX and PSA-NCAM. Three to five representative images across a minimum of three evenly spaced sections were collected for quantification at each age. Experimental replicates and different co-stains (in addition to the 3-5 sections included

for quantifications) were also analyzed for the presence of absence of young neurons or stem cells. The dentate gyrus was subdivided into regions of interest (GCL, hilus or ML) using DAPI to initially identify the cell-dense GCL. Each age has n=1. Counts for cell populations were performed by 3 separate investigators who were blinded to individual cases. For each quantified marker, counts were repeated by different investigators for reproducibility. Fluorescence signal for single reactivity and co-localization of immunoreactivity was counted individually using the markers function in the Neurolucida imaging software. The quantification of data was performed with GraphPad Prism (v6).

Electron microscopy

For transmission electron microscopy (TEM), samples were sectioned with a vibrating blade microtome (200 microns) and postfixed with 2% osmium tetroxide solution. Sections were dehydrated in increasing ethanol concentrations and stained with 2% uranyl acetate, embedded in araldite resin (Durcupan ACM Fluka, Sigma-Aldrich), and allowed to solidify at 69 °C for 72 h. We analyzed 6 control and 15 epilepsy cases via TEM. We looked for the presence of cell clusters under light and electron microscopy in the 15 epilepsy resected samples from 30 to 64 years old range (at least 15 semithin sections per case) and 4 control samples from 18-55 years old (45 semithin sections per case). In the additional control cases (7 years old and 48 years old samples) we studied 100 semithin sections spanning the entirety of the anterior to posterior levels of the DG. Ultrathin sections were obtained (70 nm) and were contrasted with lead citrate solution on grids. Pre-embedding immunohistochemistry was performed on 50-micron floating sections with DCX and Iba1 antibodies. Postfixation was performed with 7% glucose-1% Osmium tetroxide and, afterwards, followed a conventional embedding protocol. TEM micrographs of DCX immunolabeled ultrathin sections of the 22 gw (proximal edge), birth and 7 years old DG were used for the GCL cellular profiles. All images were taken at the same magnification. Cell profiles were drawn on Adobe Photoshop by following the cytoplasmic cell membranes. Cells showing DCX immunogold labeling were colored in red. DCX- cells were identified by their ultrastructural characteristics: Progenitors (light blue) had dark cytoplasm and few intermediate filaments and ensheathed DCX+ cells; Astrocytes (blue) had an irregular contour, star-shape morphology, light cytoplasm and intermediate filaments; Mature neurons showed a large cell body with a round large nucleus, and high amounts of ribosomes and organelles.

RNA scope *in situ* hybridization

Sequences of target probes, preamplifier, amplifier and label probe are proprietary and commercially available (Advanced Cell Diagnostics, Hayward, CA). Typically, the probes contain 20 ZZ probe pairs (approx. 50bp/pair) covering ~1000bp. Here, we used a probe against human DCX targeting 181-1381 of NM_000555.3 as single-plex probe. Slides for ISH were initially taken from −80°C and dried at 60°C for 1 h and fixed in 4% PFA for 2 h. After several PBS washes, slides were treated with ACD hydrogen peroxide for 10 min and then washed in water 2x before treatment in 1x target retrieval buffer (ACD) for 5 min (at 95-100°C). After washing in water and then 100% alcohol, the slides were left to dry overnight before protease treatment for 15 min at 40°C in the RNAscope oven. Hybridization of probes and amplification solutions was performed according the

manufacturer's instructions. In short, tissue sections were incubated in desired probe (~2–3 drops/section) for 2 h at 40°C. The slides were washed two times in 1x wash buffer (ACD) for 2 min each. Amplification and detection steps were performed using the RNAscope 2.5 HD Red Detection Kit reagents (ACD, 320497) for single-plex probes. Sections were incubated with Amp1 for 30 min at 40°C and then washed two times in wash buffer for 2 min each. Amp2 was incubated on the sections for 15 min at 40°C, followed by two washes in wash buffer. Sections were incubated in Amp3 for 30 min at 40°C and washed two times in wash buffer for 2 min each, followed by incubation of Amp4 for 15 min at 40°C. Slides were washed two times in wash buffer for 2 min each. Slides were incubated with Amp5 for 30 min at RT using the HybEZ humidity control tray and slide rack to maintain humidity. The slides were washed two times in 1x wash buffer for 2 min each and incubated in Amp6 for 15 min at RT before washing two times in wash buffer for 2 min each. ISH signal was detected by diluting Fast RED-B in Fast RED-A solution (1:60 ratio) and incubating sections in this solution for 10 min. Slides were washed in water 2 times to stop the reaction.

Comparative gene transcription analysis

Developmental expression data were downloaded for human hippocampus (brainspan.org; RPKM data; October 2013 release) and rhesus macaque hippocampus (blueprintnhpatlas.org; March 2014 release). To compare laser capture microdissected rhesus macaque samples to gross human hippocampus samples, we calculated average expression over all hippocampus samples for each age[33,34]. Expression data were z-score normalized for each species and ages were aligned between species based on calculated event scores of conserved timing of neurodevelopmental events[35].

Extended Data

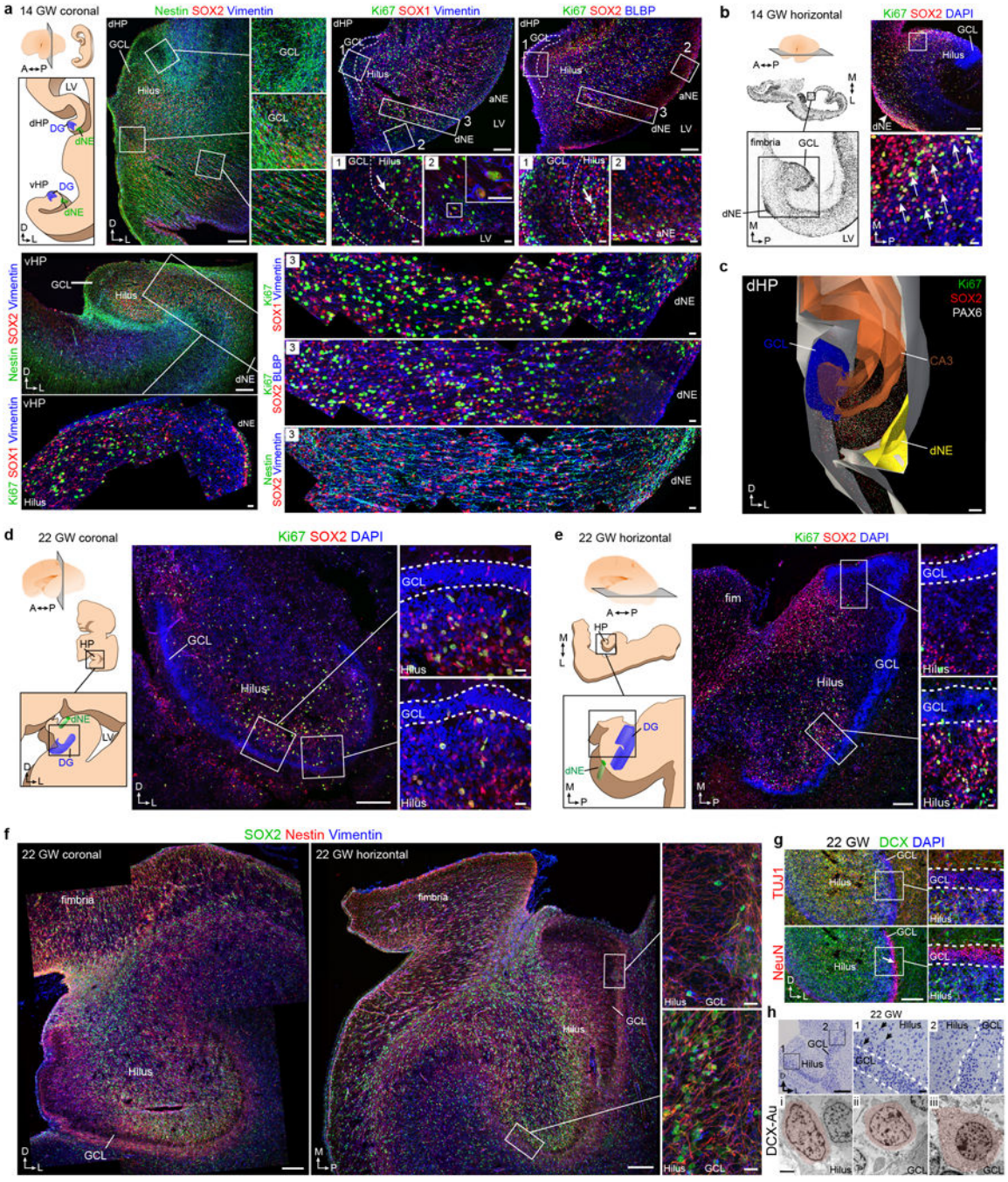

Extended Data Figure 1. Additional marker and ultrastructural analysis of early fetal development of the human dentate gyrus

a–c, 14 GW human brain **a**, schematic of dHP and vHP in a coronal section. Precursor cells labeled with Nestin, SOX2 and Vimentin are organized in ribbons between the dNE and GCL. Ki67+ cells expressing SOX1 and Vimentin or SOX2 and BLBP are present in the GCL and hilus (inset 1), along the wall of the LV (inset 2), and between the GCL and the dNE (inset 3). The dNE is located at the edge of the ammonic neuroepithelium (aNE) closest

to the fimbria. A similar organization is present in the vHP where Nestin+SOX2+Vimentin+ cells connect the dNE to the developing GCL. Ki67+SOX1+Vimentin+ cells are present in a strip along the ventricular wall and fill the region between the dNE and the GCL. **b**, (left) 14 GW hemisphere, Nissl-stained horizontal sections. (right) Ki67+ cells expressing SOX2 (arrows). **c**, 3D reconstruction of the dHP showing field of Ki67+ and SOX2+ cells between the dNE and GCL. **d–h**, 22 GW human brain, coronal (**d**) and horizontal (**e**) sections; the hilus and GCL contain Ki67+SOX2+ cells, (insets 1,2) as well as (**f**) Nestin +SOX2+Vimentin+ cells. These populations are asymmetrically distributed; sparse in the medial (proximal) GCL and hilus (inset 1) but abundant in the lateral (distal) GCL and hilus (inset 2). **g**, DCX+TUJ1+ cells and NeuN+ cells in the DG at 22 GW. NeuN+ GCL neurons in the distal GCL (arrow). **h**, Toluidine blue-stained semithin section (top) and TEM micrographs at 22 GW showing the ultrastructural characteristics of DCX immunogold labeled cells (pseudocolored, bottom). Insets of the semithin section show the proximal (1) and distal (2) ends of the GCL. Most DCX+ cells in the hilus and the proximal GCL have scant cytoplasm, few organelles, and a small, irregular nucleus (i-ii); some in the hilus have an elongated, fusiform morphology (i). Some DCX+ cells in the GCL have mature neuronal characteristics such as a round nucleus, more cytoplasm, ribosomes, rough endoplasmic reticulum and mitochondria (iii); this cell type was more common in the distal GCL. Scale bars: 200 μm (**a–h** lower magnifications), 20μm (**a–h** higher magnifications), 2 μm (**h**, TEM).

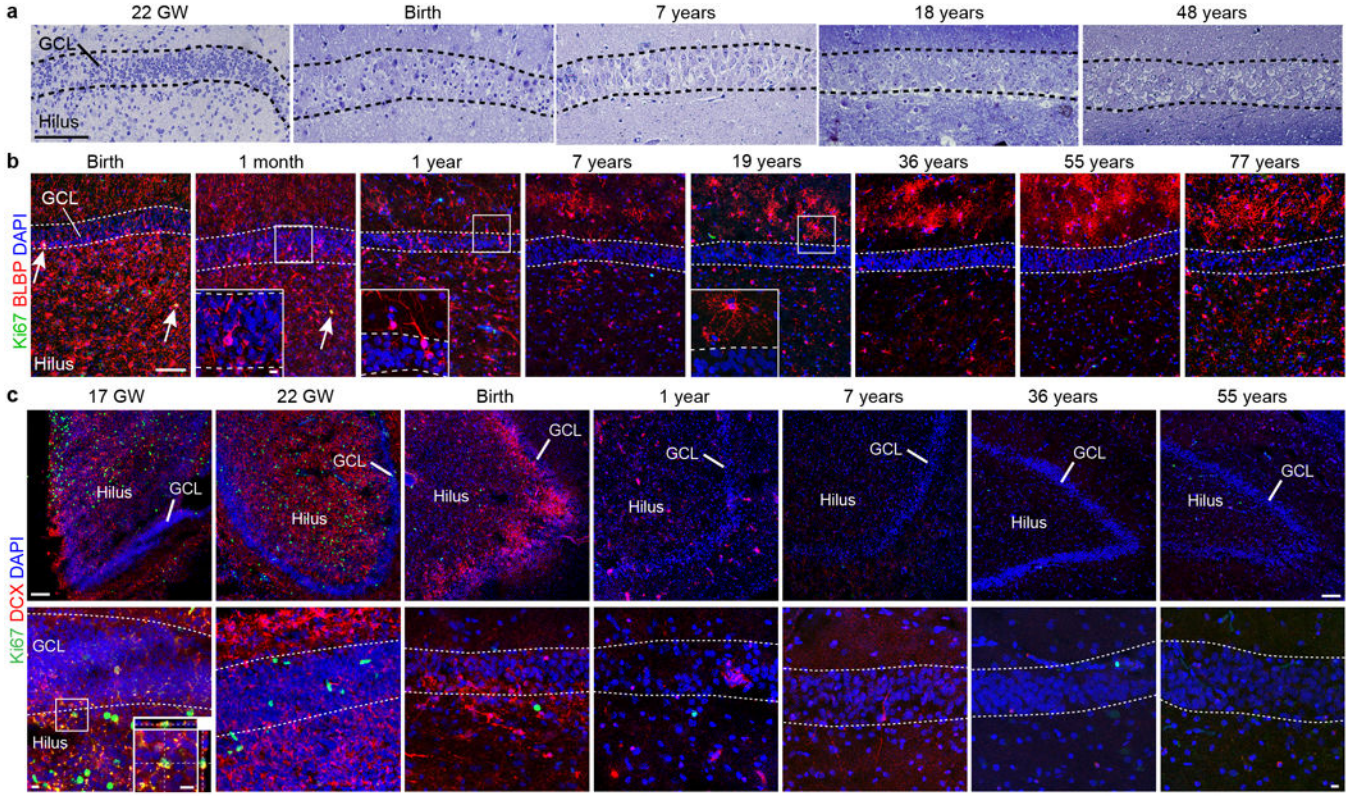

Extended Data Figure 2. A coalesced proliferative SGZ does not form in the human DG; additional marker expression

a, Toluidine blue counterstained semithin sections of the human GCL from fetal to adult ages. Note that a discrete cellular layer does not form next to the GCL and the small dark cells characteristic of SGZ precursors are not present (compare to Extended Fig. 9b in the macaque). **b**, BLBP+ cells are distributed broadly in the DG from birth to one year, many of these cells have an elongated morphology (see insets) and some co-express Ki67 (arrows) at birth and one month. By 7 years and in adults, most BLBP is present in the ML in stellate protoplasmic astrocytes. **c**, DCX+Ki67+ cells in the GCL are rare at 17 GW (orthogonal views, inset) but were abundant in the GE at the same age (not shown). DCX+Ki67+ cells were absent in the GCL from 22 GW to 55 years. Scale bars: 100 μm (**a–c**), 10μm (**a–c**, insets).

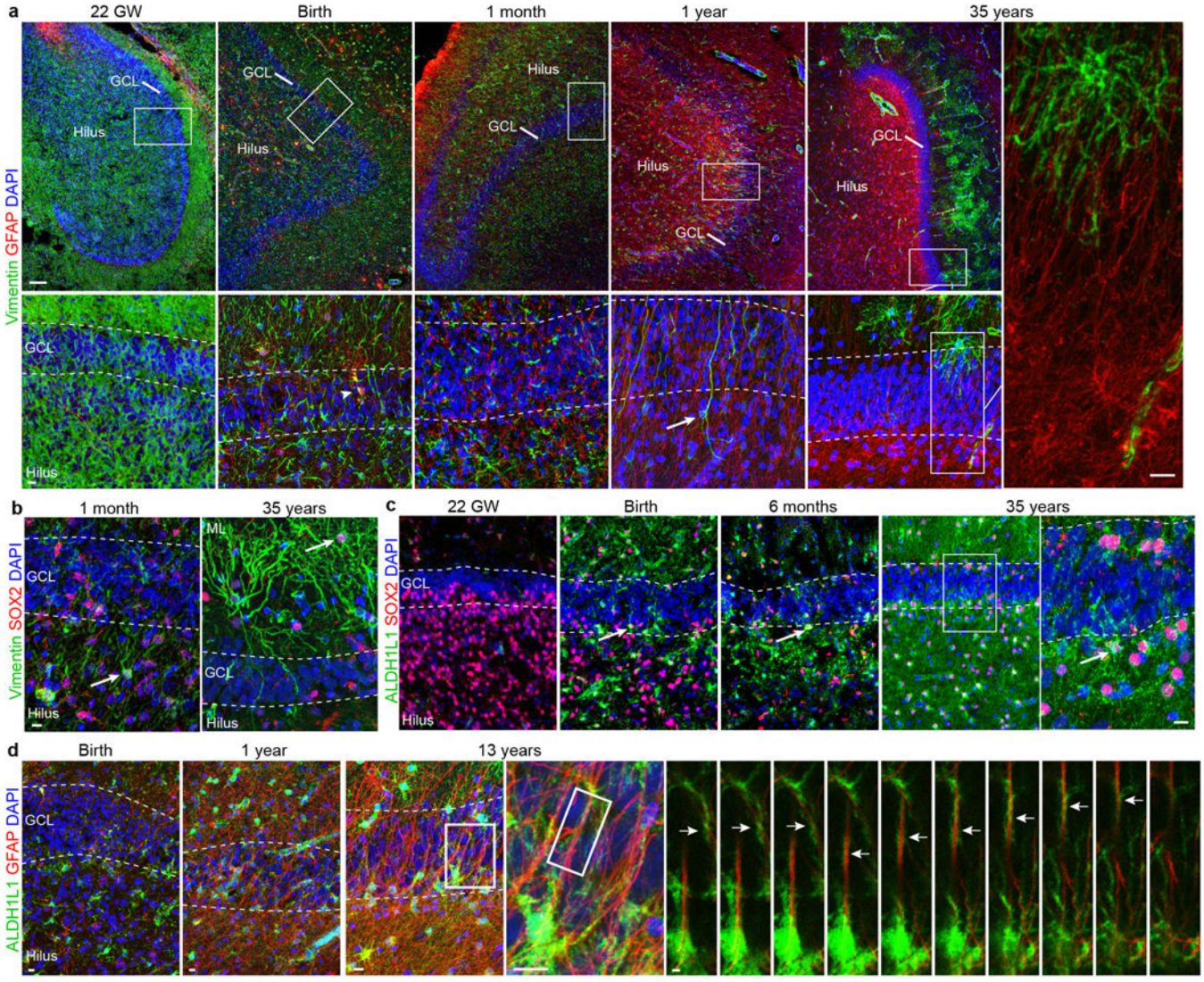

Extended Data Figure 3. Additional marker expression for astroglial cells and progenitor cells in the human DG at different ages

a, Vimentin+ and GFAP+ cells in the hippocampus from 22 gestational weeks to 35 years. Vimentin is widely expressed during fetal and early postnatal development and is mostly

restricted to protoplasmic astrocytes in the molecular layer in adults. GFAP is not expressed at 22 gestational weeks, but at birth a few vimentin+GFAP+ cells are present in the hilus and GCL (arrowhead). Interestingly, some vimentin+GFAP− cells with a radial morphology (arrow) are observed in samples at 1 year of age, but not at the other ages. In adults, GFAP and vimentin are not co-expressed (right, high-magnification of thin GFAP+vimentin− fibres within the GCL). **b**, Vimentin+Sox2+ simpler elongated cells in the hilus at 1 month (arrow) and protoplasmic astrocytes in the molecular layer at 35 years of age (arrow). **c**, SOX2+ cells are abundant in the GCL and hilus at 22 gestational weeks, and co-express ALDH1L1 in the brain at birth and in older individuals (arrows). **d**, At birth, there are few ALDH1L1+GFAP+ cells in the DG, but by 13 years of age many stellate astrocytes express both of these markers. Right, z stack of radial GFAP+ processes that are surrounded by ALDH1L1 staining. Scale bars, 100 μm (**a** (top row)), 10 μm (**a** (bottom row and insets), **b–d**) and 2 μm (**d** (z-stack)).

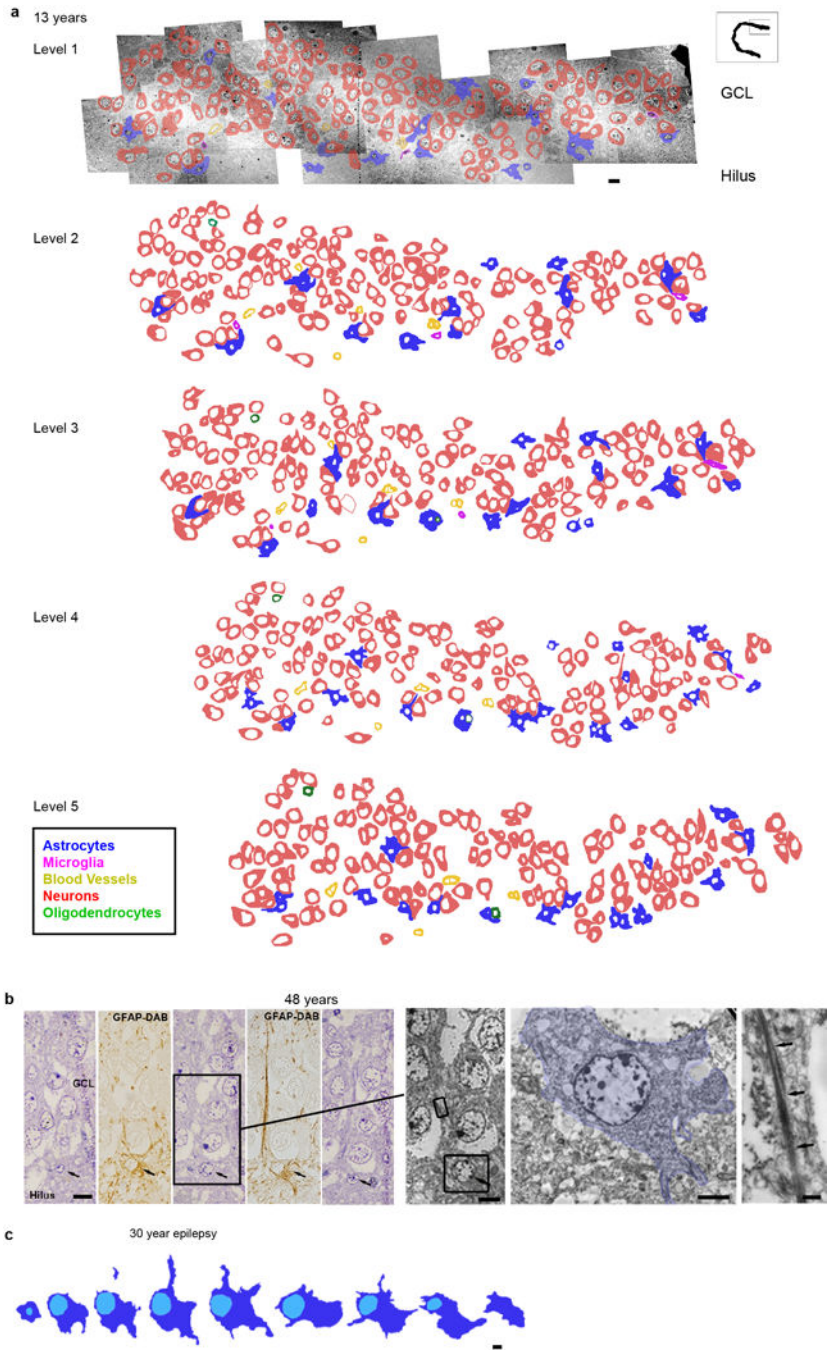

Extended Data Figure 4. EM analysis of cell types in the DG of a 13 year old and adult human brain; absence of SGZ precursor cells or immature neurons

a, Reconstruction of 5 ultrathin sections (separated by 1.5 μm) from the 13 year old GCL with outlines of cell membranes. Colors corresponding to the different cell types defined by their ultrastructural characteristics are indicated in the key. No clusters or isolated cells with young neuronal ultrastructure were found. Cells associated in small groups were identified as astrocytes, oligodendrocytes or microglia. **b–c**, reconstructions of astroglial cells next to the GCL searching for possible examples of RA in the adult human DG. **b**, example of an

astrocyte with radial morphology in the adult GCL. Five serial semithin sections of this astrocyte (black arrows) next to the GCL of a 48 year old DG ; alternating semithin sections show that this cell is GFAP+. This cell extends a thin radial fiber through the GCL, but has multiple processes (stellate morphology) in the hilus. Boxed area shows the ultrastructure from the indicated semi-thin section of this astrocyte (pseudo-coloured in blue) and the bundles of intermediate filaments present in the expansion (arrows). **c**, Another example of a serially reconstructed astrocyte in the DG of a 30 year old epileptic case (separated by 1.4 μm) showing a short radial expansion and processes into the hilus. Scale bars: 10 μm (**a, b** semithin and TEM), 5 μm (**c**), 2 μm (**b**, soma), 500 nm (**b**, intermediate filaments).

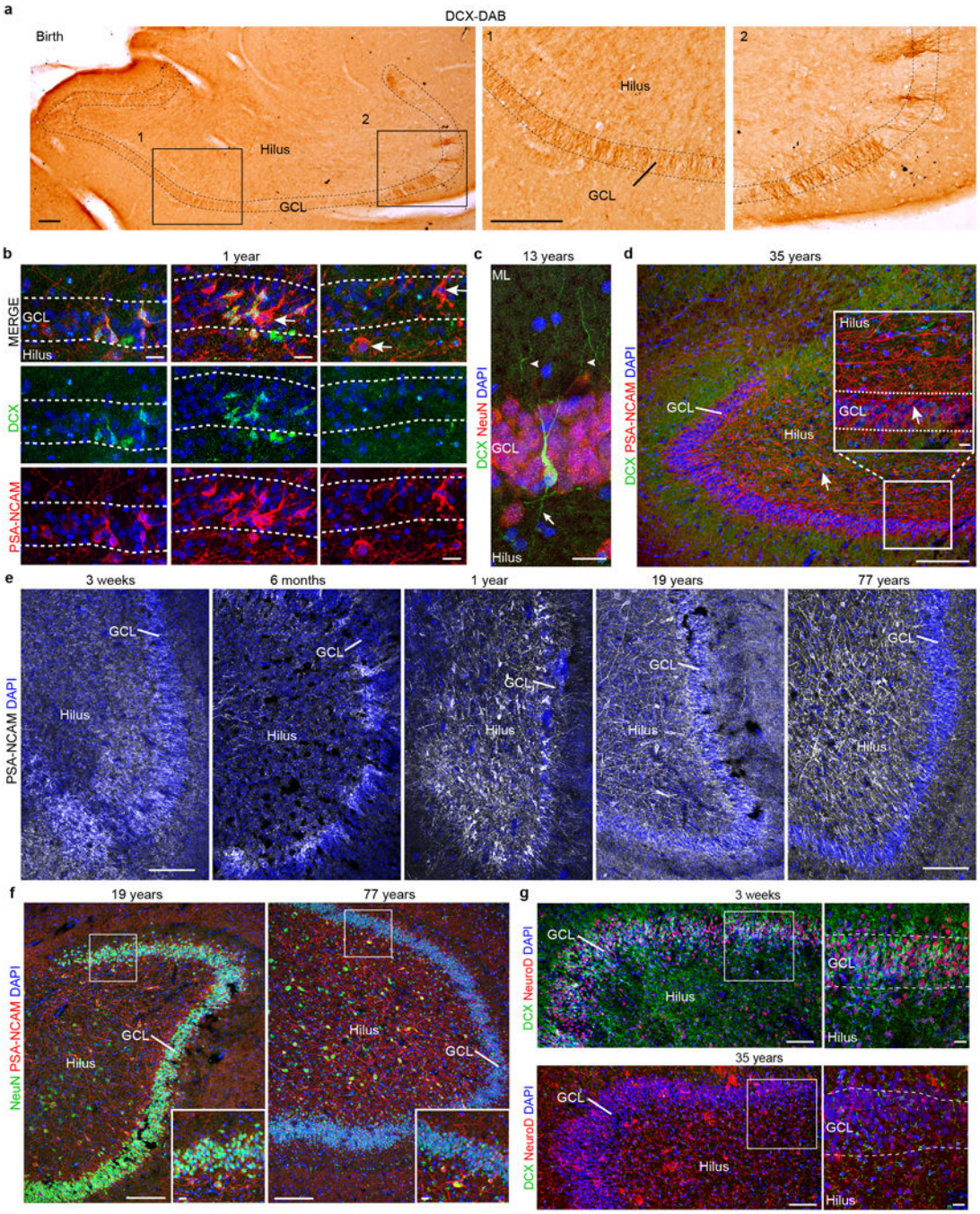

Extended Data Figure 5. Young neurons are present in the infant but not the adult human DG

a, DAB staining in the hippocampus at birth reveals many young neurons in the GCL. **b**, DCX+PSA-NCAM+ cells are distributed in clusters across the GCL at 1 year of age. Most PSA-NCAM+ cells are DCX+, but some are DCX−PSA-NCAM+ (arrows). **c**, In the samples from a 13-year-old individual, DCX+ cells have a more mature neuronal morphology. The cell shown is NeuN+ and has dendrites in the molecular layer (arrowheads) and an axon projecting into the hilus (arrow). **d**, At 35 years of age, the DG does not contain DCX+PSA-NCAM+ cells, but does contain many DCX−PSA-NCAM+

cells that do not have the morphology of young neurons. **e**, PSA-NCAM+ staining in the human DG from 3 weeks to 77 years; in adults, these cells have a more mature neuronal morphology and are localized in the hilus. **f**, PSA-NCAM+ cells in the DG are NeuN+ in samples of 19- and 77-year-old individuals. **g**, At 3 weeks of age, the GCL and hilus were filled with clusters of DCX+NeuroD+ cells, and many of the DCX− GCL neurons were NeuroD+. At 35 years, no DCX+NeuroD+ cells were observed; antibody labelling for NeuroD was non-specific. Scale bars, 200 μm (**a, d–g**), 20 μm (**b, c**, and **d, f, g** (inset)).

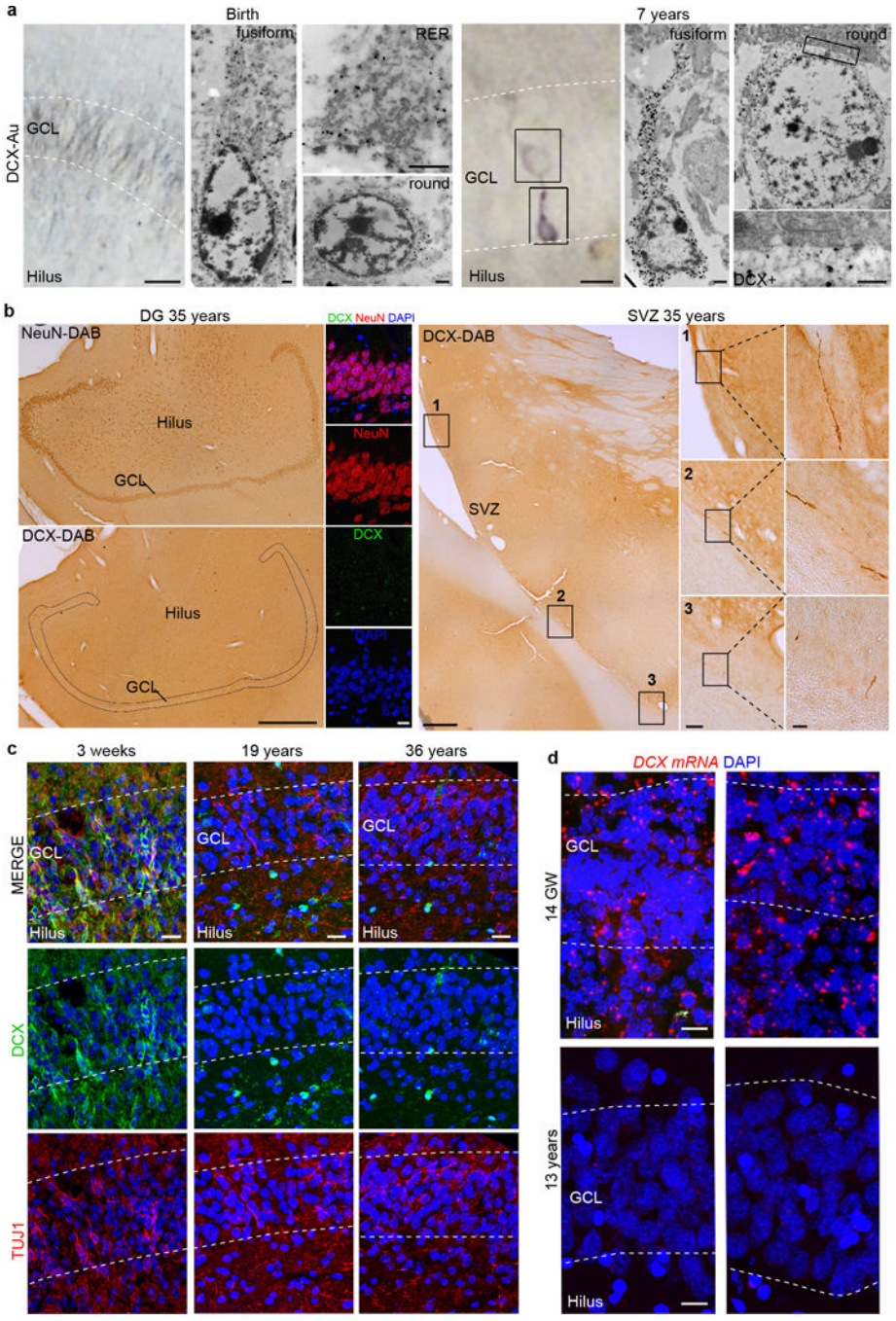

Extended Data Figure 6. DCX+ young neurons in the developing human brain, but not in the adult

a, TEM micrographs of DCX immunogold staining at birth and 7 years of age. At birth, the GCL contains small DCX+ cells with little cytoplasm, rough endoplasmic reticulum (RER) cisternae and a fusiform or round nucleus. At 7 years of age, DCX+ cells closer to the hilus have characteristics of immature neurons, including few organelles and a long expansion towards the GCL. DCX+ cells located within the GCL have mature neuron characteristics, including a large, round nucleus, rough endoplasmic reticulum, mitochondria and microtubules consistent with a more mature neuronal morphology (see Extended Data Fig. 5). At higher magnification, the more mature-appearing DCX-labelled cells are adjacent to DCX− GCL neurons. **b**, No DCX+ cells in the hilus and GCL (stained by NeuN antibodies; left insets) were found in the brain of a 35-year-old individual that showed exceptional preservation. In this sample, rare DCX+ cells with the features of young migratory neurons were present in the ventricular–subventricular zone (right insets). SVZ, subventricular zone. **c**, DCX+TUJ1+ cells were present in the GCL and hilus at 3 weeks of age, but were not detected in the adult DG. **d**, RNA-scope detection of DCX mRNA revealed many cells in the DG at 14 gestational weeks, but weakly labelled cells distributed throughout in the DG and other regions of the hippocampus at 13 years of age. Scale bars: 1 mm (b (left)), 100 μm (**b** (middle right inset)), 20 μm (**b** (right insets), **c**), 10 μm (**d**), 5 μm (**a** (left)) and 500 nm (**a** (right, TEM)).

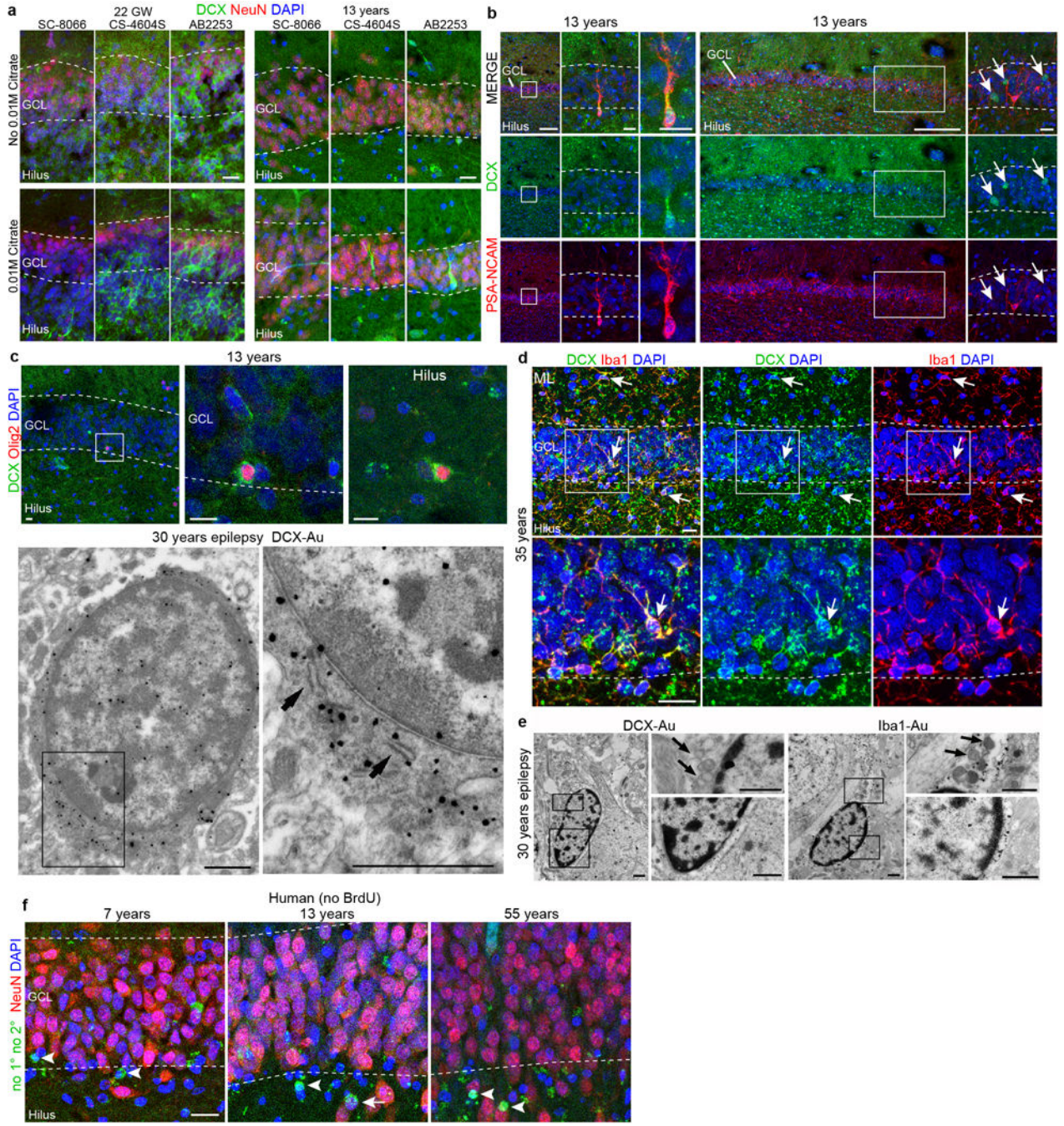

Extended Data Figure 7. DCX+/PSA-NCAM- glial cells in the adult human hippocampus

a, Comparison of citrate antigen retrieval using three DCX antibodies from this study (SC-8066, CS-4604S and AB2253) in the GCL obtained from individuals at 22 gestational weeks and 13 years of age. The 13 year old DCX+ cell (Extended Data Fig. 5c) is shown in the lower right panel and adjacent sections were stained with the other antibodies. **b**, Example of a DCX+PSA-NCAM+ neuron in the GCL and DCX+PSA-NCAM− staining in the sample from the 13-year-old individual (arrows). **c**, Examples of DCX+OLIG2+ cells in the GCL and hilus of the 13-year-old individual. Immunogold-labelled DCX+ cells viewed

by TEM had single short endoplasmic reticulum cisternae (arrows), a very irregular contoured membrane and a round nucleus with condensed chromatin characteristic of oligodendrocytes. **d**, In some samples (see Extended Data Fig. 5g, bottom right inset), we found DCX+ immunoreactivity in many small multipolar cells. This staining was not limited to the hilus, or GCL, but was present in cells across the tissue and co-localized with the microglial marker IBA1 (arrows). e, TEM micrographs of DCX and IBA1 immunogold-labelled cells in an adult DG of a 30-year-old individual with epilepsy. DCX+ and IBA1+ cells have similar characteristics: elongated nucleus with clumps of chromatin beneath the nuclear envelope and throughout the nucleoplasm, irregular contour and the presence of lysosomes and lipofucsin (arrows). Note that these features are typical of microglial cells. **f**, Human hippocampus stained with NeuN followed by processing for BrdU detection (with no primary or secondary antibodies) shows round fluorescent signal (arrowheads indicate signal that is NeuN−) occasionally overlapping with NeuN staining (arrow). Scale bars, 200 μm (**b** (left column and wide column)), 20 μm (**a, b** (left-middle columns, right column), **d, f**), 10 μm (**c** (top row)) and 1 μm (**c** (bottom row), **e**).

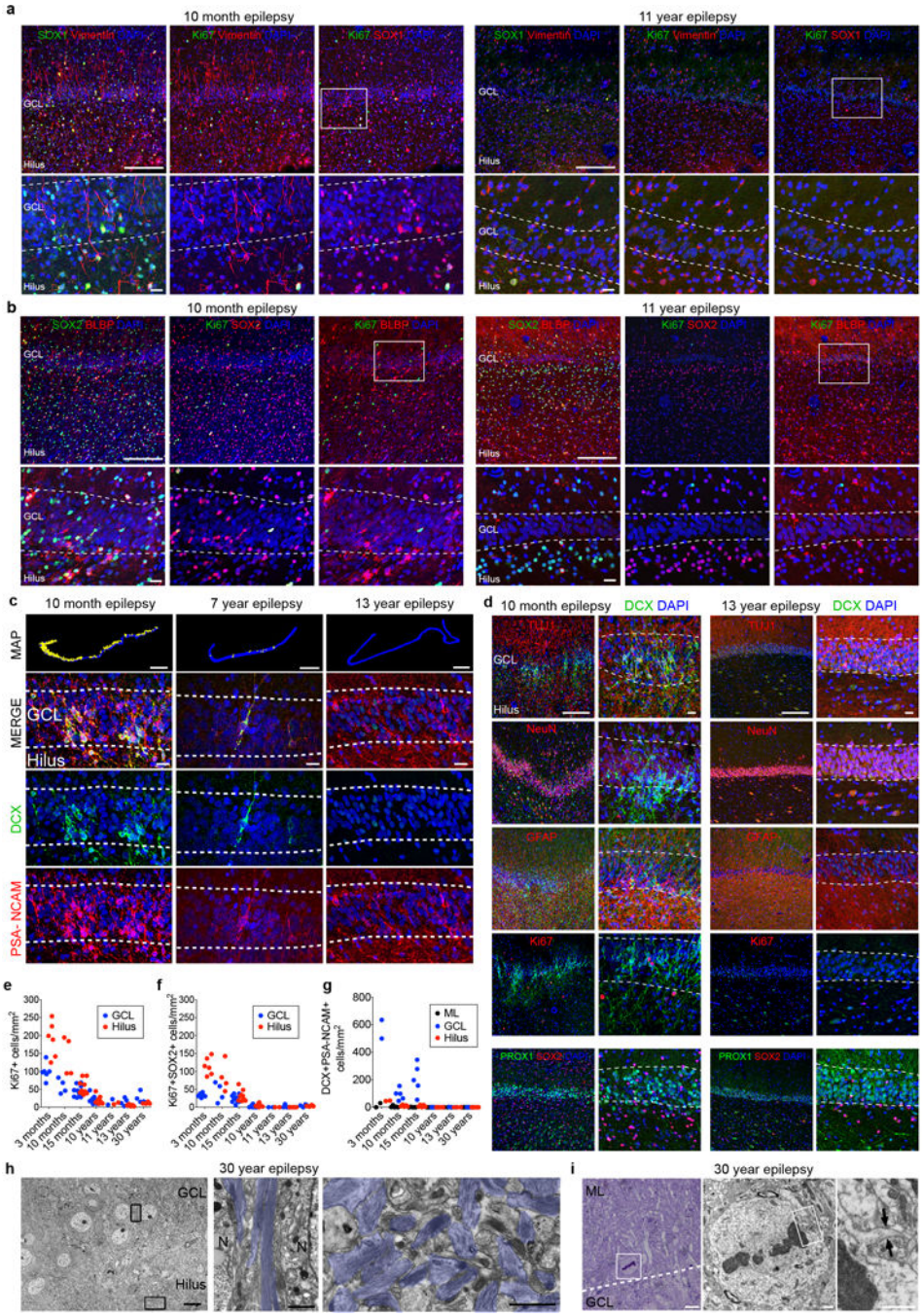

Extended Data Figure 8. Neurogenesis declines in epilepsy cases from infancy into childhood

a, Ki-67+SOX1+vimentin+ cells are located in the hilus and GCL at 10 months but are not present at 11 years of age. **b**, Ki-67+SOX2+BLBP+ cells are located in the hilus and GCL at 10 months but are not present at 11 years of age. **c**, Maps of DCX+PSA-NCAM+ cells (yellow dots) and representative immunostaining at 10 months, 7 years and 13 years (bottom rows). **d**, In the 10 month-old epileptic DG of a patient with epilepsy, DCX+ cells co-expressing PSA-NCAM or TUJ1 are distributed throughout the NeuN+PROX1+ GCL, but do not co-express Ki-67 or GFAP. In the 13-year-old patient with epilepsy, DCX+ cells co-

expressing PSA-NCAM or TUJ1 were not present. Few Ki-67+ cells were visible throughout the DG. **e–g**, Quantification of Ki-67+ (**e**), Ki-67+SOX2+ (**f**) and DCX+PSA-NCAM+ (**g**) cells in the DG of surgically resected hippocampuses. **h**, TEM micrographs of the brain of a 30-year-old patient with epilepsy showing astroglial expansions with high number of intermediate filaments (blue) ensheathing GCL neuronal bodies. A dense network of astrocytic expansions in the hilus, containing dense bundles of intermediate filaments (blue), fills the region proximal to the GCL with no evidence of SGZ progenitor cells. **i**, Mitotic cells are very rare and not restricted to the hilus or GCL. A toluidine-blue-stained 1.5-μm section from the DG of a 30-year-old brain shows a dividing cell in the molecular layer, adjacent to the GCL. The TEM micrograph shows the dividing cell in metaphase with a light cytoplasm, few organelles and an irregular contour with a small expansion (arrows), which are characteristic of astrocytes (shown at higher magnification). N, neuron. For quantifications, staining replicates (≥3) are shown by dots (each age, n = 1). Scale bars, 1 mm (**c** (maps)), 200 μm (**a, b** (top), **d** (left)), 20 μm (**a–c** (bottom), **d** (right)) and 10 μm (**h, i** (left)), 1 μm (**h, i** (middle and right)).

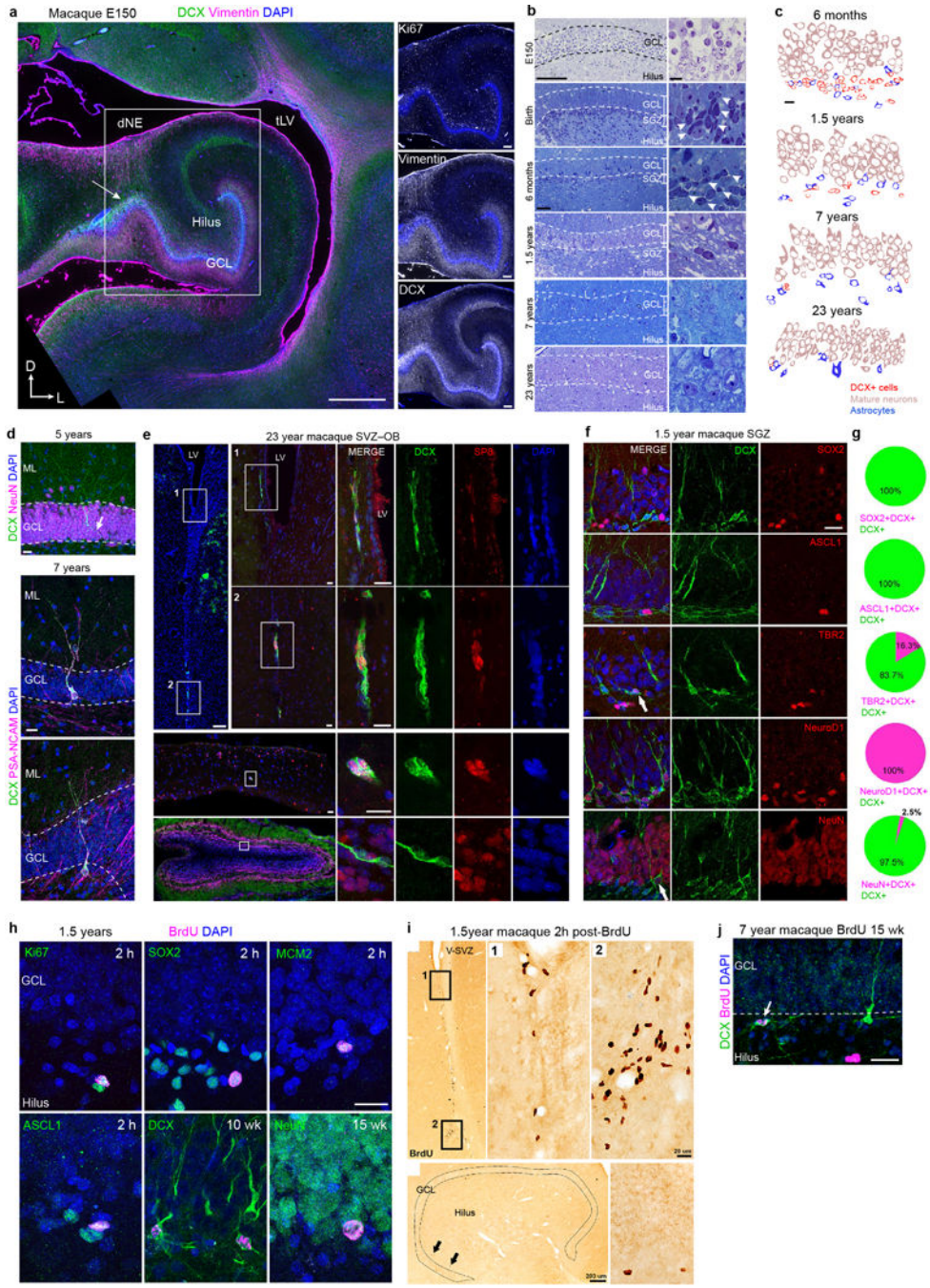

Extended Data Figure 9. Development of the macaque DG and evidence for the presence of a proliferative SGZ and postnatal neurogenesis with a sharp decline in adulthood

a, The E150 macaque hippocampus has many Ki67+ cells in the SGZ as well as Vimentin+ fibers and DCX+ cells between the dNE and the GCL (arrow). **b**, Toluidine blue-stained semi-thin sections of the macaque DG reveal small and darkly condensed nuclei (arrows) in the SGZ from fetal ages (E150) to 1.5 years; few are visible at 7 and these cells are very rare in the 23 year macaque DG (compare with human data in Extended Data Fig. 2a). **c**, Profiles of the cellular populations in the macaque DG at 6 months, 1.5 years, 7 years, and 23 years

of age. As in the human DG, DCX+ cells decrease dramatically with age and have scarce cytoplasm and a smaller nucleus compared to mature granule neurons. **d**, (top) Example of a DCX+NeuN+ cell with mature dendrites in the macaque GCL at 5 years of age. (middle, bottom) Two examples of DCX+PSA-NCAM+ cells with dendritic arborization present in the macaque GCL at 7.5 years of age. An axonal extension (arrow) into the hilus is visible. **e**, The 23 year old macaque V-SVZ and olfactory bulb (OB) contain some DCX+SP8+ cells with morphology of young neurons, but similar cells are rare in the 23 year old GCL in the hippocampus (ig. 4b, d) **f**, DCX+ cells in the 1.5 year old macaque SGZ express transcription factors in common with those in the mouse SGZ. **g**, Percentages of DCX+ cells expressing markers in (**f**). **h**, Immunostains of BrdU+ cells and cell proliferation (Ki67, MCM2), progenitor cell markers (Sox2, Ascl1) or DCX, in the 1.5 year-old macaque sacrificed at 2 hours after BrdU injection. BrdU+DCX+ and BrdU+NeuN+ cells could be identified at 10 or 15 weeks after BrdU exposure, respectively. **i**, DAB-staining for BrdU in the 1.5 year old macaque V-SVZ and SGZ, 2 hours after BrdU. **j**, Example of a rare DCX +BrdU+ cell in the 7.5 year old macaque. Scale bars: 1 mm (**a** left) 200 μm (**a** right, **e** top left, bottom left, **i**, left), 100 μm (**b**, left) 20 μm (**d, e** middle left and right, **f,h, i** right, **j**), 10 μm (**b**, right, **c**).

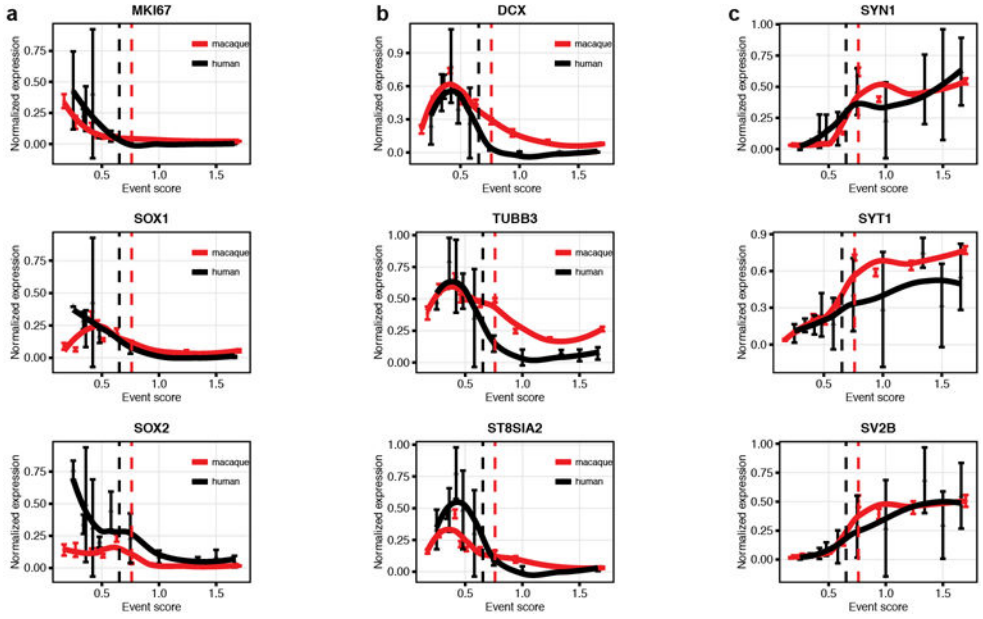

Extended Data Figure 10. Decline in markers associated with neurogenesis in the macaque and human hippocampus (gene expression profiling)

a, markers of dividing or precursor cells **b**, markers of young neurons **c**, markers of mature neurons. Human RNAseq (brainspan.org) and macaque expression profiling (data set from Bakken et al. 2016) developmental data from hippocampus for the indicated genes. Human data are averaged over biological replicates by developmental period (as defined by Kang et al. 2011). Normalized data are plotted on the same developmental event scale. Loess-fit curves are displayed with data points (mean +/− sem). Dashed lines indicate birth.

Supplementary Material

Refer to Web version on PubMed Central for supplementary material.

Acknowledgments

We thank the families who graciously donated the tissue samples used in this study, and Jose Rodriguez, Vivian Tang, Jennifer Cotter and Cristina Guinto for technical support. S.F.S. was supported by F32 MH103003 and M.F.P. was supported by K08 NS091537. A. A.-B. was supported by NIH grants P01 NS083513, R01 NS028478 and a generous gift from the John G. Bowes Research Fund. He is the Heather and Melanie Muss Endowed Chair and Professor of Neurological Surgery at UCSF and is a co-founder and serves on the scientific advisory board of Neurona Therapeutics. G.W.M. was partly supported by the Davies/Crandall Endowed Chair For Epilepsy Research at UCLA. G.W.M. and J.C. was supported by NIH NINDS (NS083823 and U01 MH108898). M.C.O. was supported by a Scholar Award from the UCSF Weill Institute for Neurosciences. We acknowledge NSFC grants to Z. Yang (31425011, 31630032, and 31421091). S.M. was supported by the European Molecular Biology Organization (EMBO) Long term fellowship. J.M.G.-V. and A.C.S. were supported by MINECO/FEDER Grant BFU2015-64207-P, Red de Terapia Celular TerCel, Instituto de Salud Carlos III (ISCIII2012-RED-19-016 and RD12/0019/0028) and PROMETEOII/2014/075.

References

1. Altman J, Das GD. Autoradiographic and histological evidence of postnatal hippocampal neurogenesis in rats. J Comp Neurol. 1965; 124:319–335. [PubMed: 5861717]
2. Kornack DR, Rakic P. Continuation of neurogenesis in the hippocampus of the adult macaque monkey. Proc Natl Acad Sci U S A. 1999; 96:5768–5773. [PubMed: 10318959]
3. Seri B, García-Verdugo JM, McEwen BS, Alvarez-Buylla A. Astrocytes give rise to new neurons in the adult mammalian hippocampus. J Neurosci. 2001; 21:7153–7160. [PubMed: 11549726]
4. van Praag H, et al. Functional neurogenesis in the adult hippocampus. Nature. 2002; 415:1030–1034. [PubMed: 11875571]
5. Patzke N, et al. In contrast to many other mammals, cetaceans have relatively small hippocampi that appear to lack adult neurogenesis. Brain Struct Funct. 2015; 220:361–383. [PubMed: 24178679]
6. Kempermann G, Kuhn HG, Gage FH. More hippocampal neurons in adult mice living in an enriched environment. Nature. 1997; 386:493–495. [PubMed: 9087407]
7. van Praag H, Kempermann G, Gage FH. Running increases cell proliferation and neurogenesis in the adult mouse dentate gyrus. Nat Neurosci. 1999; 2:266–270. [PubMed: 10195220]
8. Lugert S, et al. Quiescent and active hippocampal neural stem cells with distinct morphologies respond selectively to physiological and pathological stimuli and aging. Cell Stem Cell. 2010; 6:445–456. [PubMed: 20452319]
9. Malberg JE, Duman RS. Cell proliferation in adult hippocampus is decreased by inescapable stress: reversal by fluoxetine treatment. Neuropsychopharmacology. 2003; 28:1562–1571. [PubMed: 12838272]
10. Hill AS, Sahay A, Hen R. Increasing Adult Hippocampal Neurogenesis is Sufficient to Reduce Anxiety and Depression-Like Behaviors. Neuropsychopharmacology. 2015; 40:2368–2378. [PubMed: 25833129]
11. Spalding KL, et al. Dynamics of hippocampal neurogenesis in adult humans. Cell. 2013; 153:1219–1227. [PubMed: 23746839]
12. Dennis CV, Suh LS, Rodriguez ML, Kril JJ, Sutherland GT. Human adult neurogenesis across the ages: An immunohistochemical study. Neuropathol Appl Neurobiol. 2016; 42:621–638. [PubMed: 27424496]
13. Eriksson PS, et al. Neurogenesis in the adult human hippocampus. Nat Med. 1998; 4:1313–1317. [PubMed: 9809557]
14. Knoth R, et al. Murine features of neurogenesis in the human hippocampus across the lifespan from 0 to 100 years. PLoS One. 2010; 5:e8809. [PubMed: 20126454]
15. Yang P, et al. Developmental profile of neurogenesis in prenatal human hippocampus: an immunohistochemical study. Int J Dev Neurosci. 2014; 38:1–9. [PubMed: 24999120]

16. Venere M, et al. Sox1 marks an activated neural stem/progenitor cell in the hippocampus. Development. 2012; 139:3938–3949. [PubMed: 22992951]
17. Suh H, et al. In vivo fate analysis reveals the multipotent and self-renewal capacities of Sox2+ neural stem cells in the adult hippocampus. Cell Stem Cell. 2007; 1:515–528. [PubMed: 18371391]
18. Steiner B, et al. Type-2 cells as link between glial and neuronal lineage in adult hippocampal neurogenesis. Glia. 2006; 54:805–814. [PubMed: 16958090]
19. Sanai N, et al. Corridors of migrating neurons in the human brain and their decline during infancy. Nature. 2011; 478:382–386. [PubMed: 21964341]
20. Wang C, et al. Identification and characterization of neuroblasts in the subventricular zone and rostral migratory stream of the adult human brain. Cell Res. 2011; 21:1534–1550. [PubMed: 21577236]
21. Gould E, et al. Hippocampal neurogenesis in adult Old World primates. Proc Natl Acad Sci U S A. 1999; 96:5263–5267. [PubMed: 10220454]
22. Kornack DR, Rakic P. The generation, migration, and differentiation of olfactory neurons in the adult primate brain. Proc Natl Acad Sci U S A. 2001; 98:4752–4757. [PubMed: 11296302]
23. Sugiyama T, Osumi N, Katsuyama Y. The germinal matrices in the developing dentate gyrus are composed of neuronal progenitors at distinct differentiation stages. Dev Dyn. 2013; 242:1442–1453. [PubMed: 24038449]
24. Altman J, Bayer SA. Mosaic organization of the hippocampal neuroepithelium and the multiple germinal sources of dentate granule cells. J Comp Neurol. 1990; 301:325–342. [PubMed: 2262594]
25. Komitova M, Eriksson PS. Sox-2 is expressed by neural progenitors and astroglia in the adult rat brain. Neurosci Lett. 2004; 369:24–27. [PubMed: 15380301]
26. Zhang Y, et al. An RNA-sequencing transcriptome and splicing database of glia, neurons, and vascular cells of the cerebral cortex. J Neurosci. 2014; 34:11929–11947. [PubMed: 25186741]
27. Breunig JJ, Arellano JI, Macklis JD, Rakic P. Everything that glitters isn't gold: a critical review of postnatal neural precursor analyses. Cell Stem Cell. 2007; 1:612–627. [PubMed: 18371403]
28. Gould E. How widespread is adult neurogenesis in mammals. Nat Rev Neurosci. 2007; 8:481–488. [PubMed: 17514200]
29. Mathews KJ, et al. Evidence for reduced neurogenesis in the aging human hippocampus despite stable stem cell markers. Aging Cell. 2017; doi: 10.1111/acel.12641
30. Fahrner A, et al. Granule cell dispersion is not accompanied by enhanced neurogenesis in temporal lobe epilepsy patients. Exp Neurol. 2007; 203:320–332. [PubMed: 17049346]
31. Eckenhoff MF, Rakic P. Nature and fate of proliferative cells in the hippocampal dentate gyrus during the life span of the rhesus monkey. J Neurosci. 1988; 8:2729–2747. [PubMed: 3411351]
32. Mathern GW, et al. Seizures Decrease Postnatal Neurogenesis and Granule Cell Development in the Human Fascia tDentata. Epilepsia. 2002; 43:68–73.
33. Bakken TE, et al. A comprehensive transcriptional map of primate brain development. Nature. 2016; 535:367–375. [PubMed: 27409810]
34. Kang HJ, et al. Spatio-temporal transcriptome of the human brain. Nature. 2011; 478:483–489. [PubMed: 22031440]
35. Workman AD, Charvet CJ, Clancy B, Darlington RB, Finlay BL. Modeling transformations of neurodevelopmental sequences across mammalian species. J Neurosci. 2013; 33:7368–7383. [PubMed: 23616543]

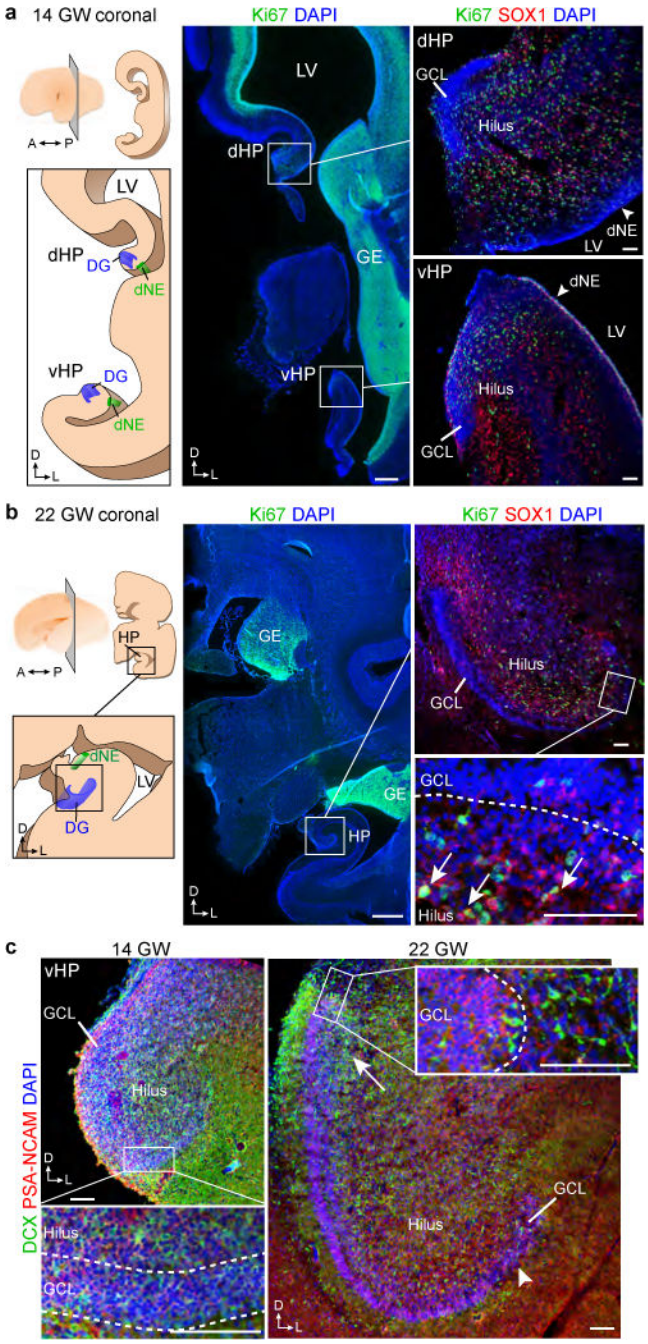

Figure 1. Early fetal development of the human dentate gyrus

a, Left, schematic of one hemisphere at 14 gestational weeks (GW), coronal section showing the lateral ventricle (LV) and ganglionic eminence (GE). Middle and right, immunofluorescence images. Ki-67+SOX1+ cells were found in the dorsal (dHP) and ventral (vHP) hippocampus. A, anterior; D, dorsal, L, lateral; P, posterior. **b**, Left, schematic of one hemisphere at 22 gestational weeks, coronal section. Middle and right, SOX1+Ki-67+ cells in the hilus and GCL (arrows). **c**, Distribution of DCX+PSA-NCAM+ cells at 14 gestational weeks and 22 gestational weeks. The arrow indicates the end of the GCL most

proximal to the dNE. The distal end of the GCL contained fewer young neurons (arrowhead). Scale bars, 1 mm (**a, b** (middle)) and 100 μm (**a, b** (right), **c**). Staining was replicated at least three times (n = 1 at 14 gestational weeks; n = 3 at 22 gestational weeks).

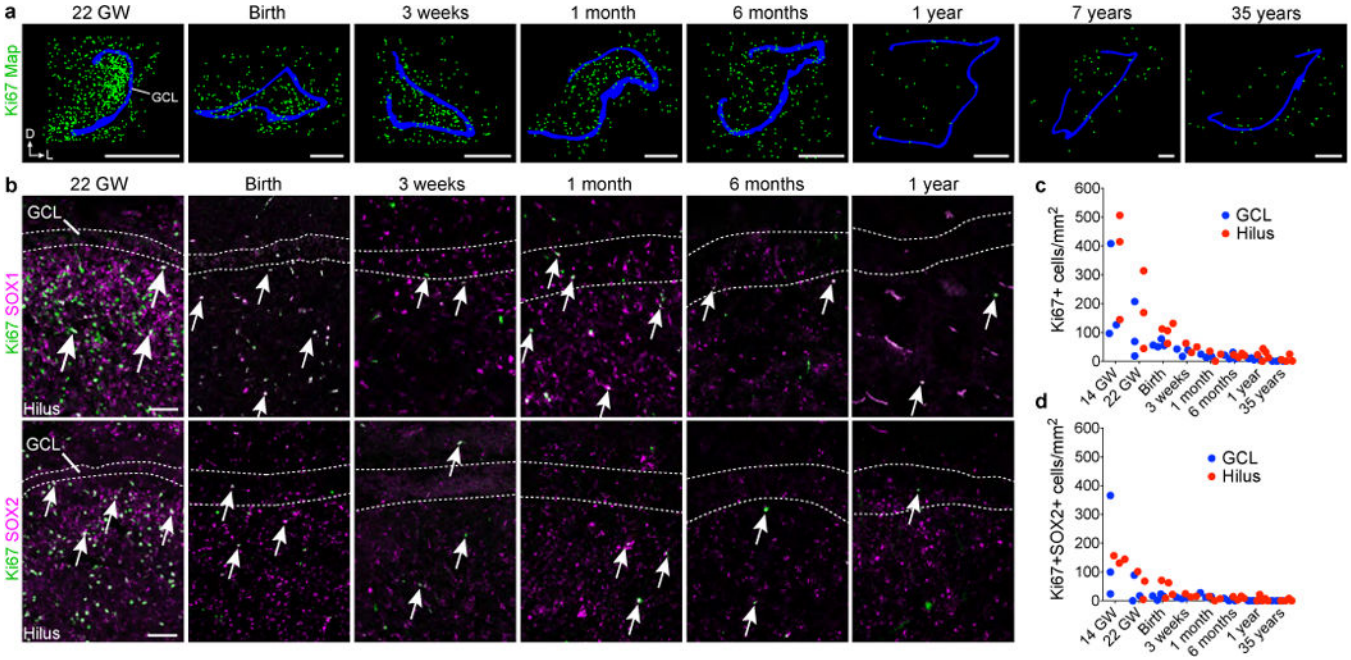

Figure 2. Human DG proliferation declines sharply during infancy and a layer of proliferating progenitors does not form in the SGZ

a, Maps of Ki-67+ (green) cells in the DG from samples of individuals that were between 22 gestational weeks and 35 years of age; GCL in blue. **b**, Ki-67+SOX1+ and Ki-67+SOX2+ cells (arrows) are distributed across the hilus and GCL and the number of double-positive cells decreases between 22 gestational weeks and 1 year of age. **c, d**, Quantification of Ki-67+ (**c**) and Ki-67+SOX2+ (**d**) cells in the hilus and GCL. For quantifications, dots indicate staining replicates (≥3) (each age n = 1). Scale bars, 1 mm (**a**) and 100 μm (**b**).

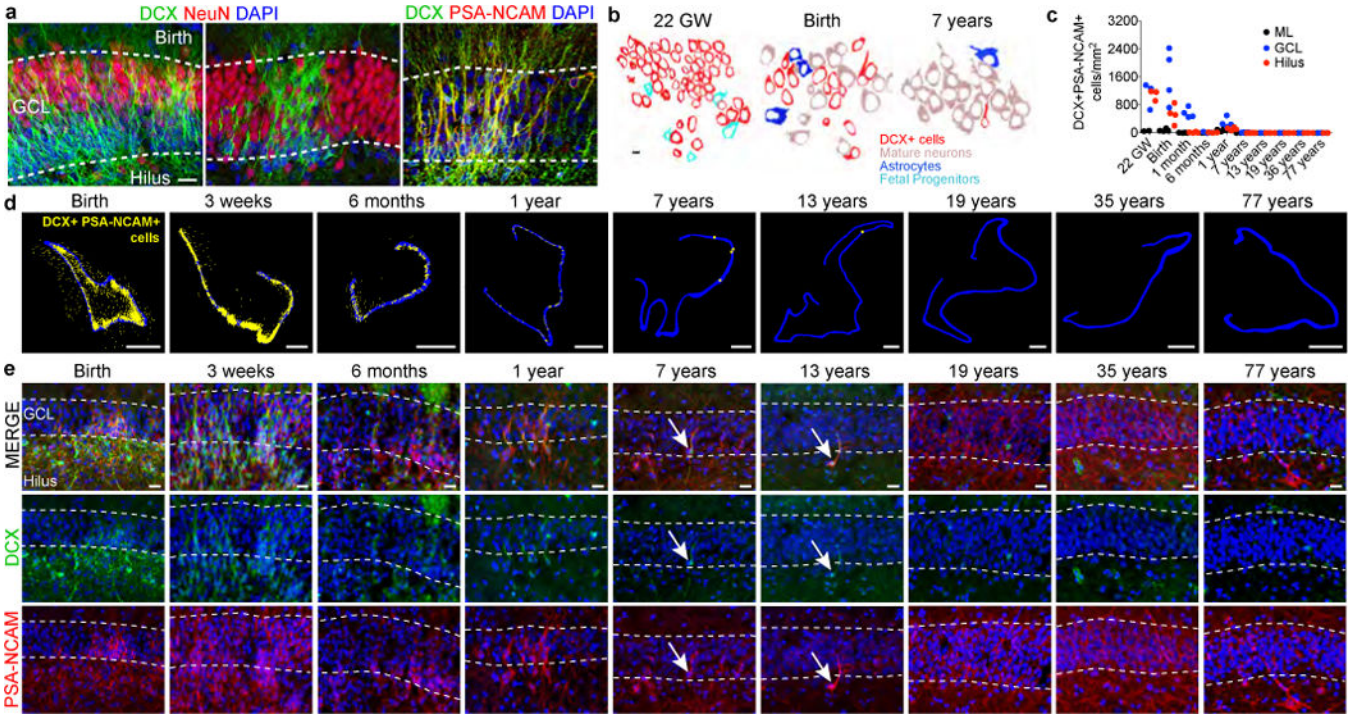

Figure 3. Young neurons decline in the human DG from infancy into childhood

a, DCX+ cells at birth are distributed in a continuous field (left) or tight clusters (middle) and express PSA-NCAM (right). **b**, Outlines of cell types in the GCL at 22 gestational weeks, birth and 7 years of age. **c**, Quantification of DCX+PSA-NCAM+ cells in the DG. **d**, Maps of DCX+PSA-NCAM+ cells (yellow dots; GCL, blue outline). **e**, DCX+PSA-NCAM + cells in the DG (birth to 77 years) are rare by 7 and 13 years of age (arrows). For quantifications, dots indicate staining replicates (≥3) (each age, n = 1). Scale bars, 1 mm (**d**), 20 μm (**a, e**) and 5 μm (**b**).

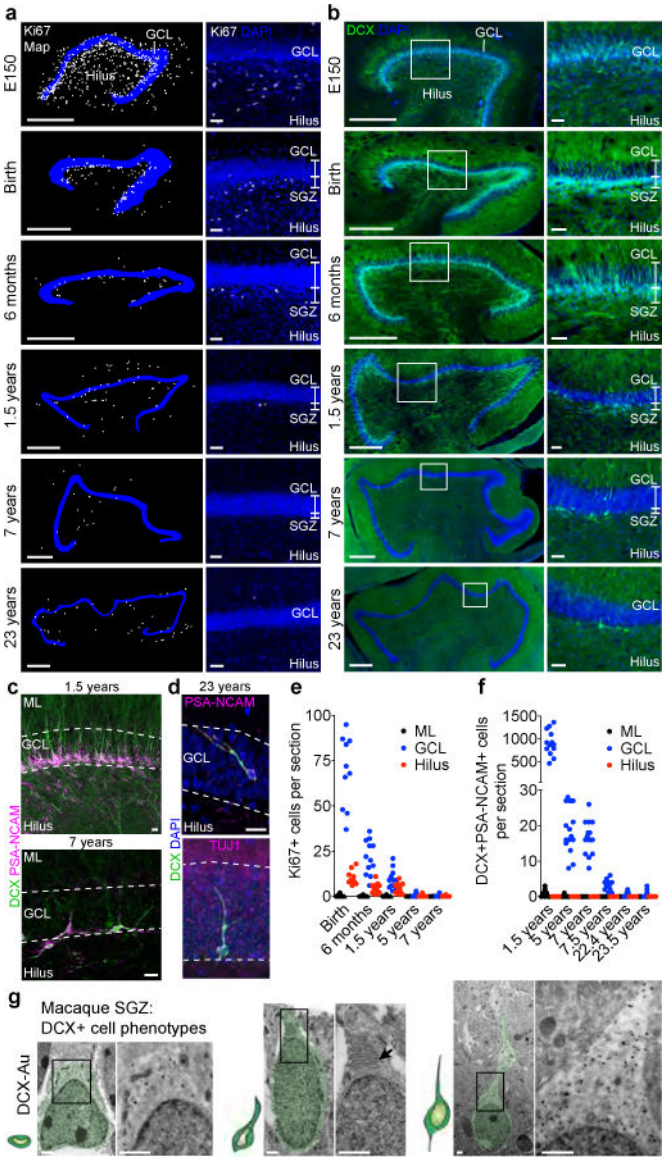

Figure 4. An SGZ forms during macaque development but new neurons are rare in adults

a, b, Maps and immunostaining of Ki-67+ cells (a) and DCX+ cells (**b**) in the macaque SGZ (from E150 to 23 years of age). **c**, DCX+PSA-NCAM+ cells in the SGZ (1.5 and 7 years). **d**, DCX+PSA-NCAM+ or DCX+TUJ1+ cells (23 years). **e, f**, Quantification of Ki-67+ cells (**e**) and DCX+PSA-NCAM+ cells (**f**) in the macaque GCL, hilus and molecular layer (ML). n = 1 animal per age; dots indicate staining replicates (≥3). **g**, Immunogold (DCX–Au) transmission electron microscopy of neurons (light green overlay) at different stages of maturation. Left, small DCX+ cell; middle, DCX+ cell with a short process, mitochondria and prominent endoplasmic reticulum (arrow); right, large DCX+ cell with round soma, few organelles and an expansion into the GCL. Scale bars, 500 μm (**a, b** (left)), 50 μm (**a, b** (right)), 20 μm (**c, d**) and 1 μm (**g**).